ISSN 0735-1097/04/$30.00
doi:10.1016/j.jacc.2004.07.055

PRECLINICAL RESEARCH

Moderate and Chronic Hemodynamic Overload of Sheep Atria Induces Reversible Cellular Electrophysiologic Abnormalities and Atrial Vulnerability

Edith Deroubaix, PHD,* Thierry Folliguet, MD,† Catherine Rücker-Martin, PHD,* Sylvie Dinanian, MD,‡ Christophe Boixel, PHD,§ Pierre Validire, MD,† Pierre Daniel, DVM,† André Capderou, MD, PHD,* Stéphane N. Hatem, MD, PHD§

Paris, Le Plessis-Robinson, and Clamart, France

OBJECTIVES The aim of this study was to evaluate the myocardial consequences of a chronic volume overload of the left atrium (LA).

BACKGROUND Atrial dilation is a major risk factor for atrial fibrillation (AF), but the underlying mechanisms are poorly understood.

METHODS A left-right aorto-pulmonary artery shunt (APS) was created in sheep. The cardiopathy was characterized by echocardiography, electrophysiologic testing, and histologic analysis. Cellular action potential (AP) and calcium current (I_{Ca}) were recorded by means of microelectrode and patch clamp techniques.

RESULTS Three to four months after surgery, all animals in the APS state had a dilated LA (146.2 ± 35.4 cm^2/m^2 vs. 91.7 ± 10.4 cm^2/m^2 in the control state; $p = 0.0024$) but remained in sinus rhythm. Repetitive atrial firing was triggered by a single extra beat in five of six animals in the APS state and in two of six animals in the control state. Moreover, in two animals in the APS state, a single extra beat triggered sustained AF. Myocytes were enlarged and 39.8% showed some degree of myolysis. In animals in the APS state, the AP had no plateau phase or small amplitude and numerous myocytes were unexcitable. The I_{Ca} density was 45.2% lower in APS animals than in control animals. Beta-adrenergic stimulation normalized I_{Ca} and restored the plateau phase of the AP. After shunt suppression, the electrophysiologic properties of the atria returned to normal.

CONCLUSIONS The APS induced moderate, isolated LA dilation, which was sufficient to cause major changes in cellular electrophysiologic properties and to render the atria vulnerable to fibrillation. These effects were reversed by shunt suppression. (J Am Coll Cardiol 2004;44: 1918–26) © 2004 by the American College of Cardiology Foundation

Atrial fibrillation (AF), the most frequent cardiac arrhythmia encountered in clinical practice, is often associated with cardiopathies complicated by hemodynamic overload of the atria, such as congestive heart failure (CHF) and mitral valve diseases (1). Moreover, the clinical association of AF with atrial enlargement has long been recognized (2). A number of studies have focused on the pathogenesis of susceptibility to AF in dilated atria (3). For instance, acute atrial dilation considerably shortens action potential (AP) duration by activating mechano-sensitive mechanisms (4). In contrast, the pathogenesis of vulnerability to AF in chronic atrial dilation remains poorly understood, probably owing to the scarcity of experimental models (5–9). Dilated right human atria have a short AP and a brief cellular effective refractory period (ERP), as observed during AF, suggesting that changes in electrical properties may precede arrhythmia and contribute to susceptibility to AF (10). However, in dogs with mitral valve disease and chronic atrial dilation, cellular electrical properties are only slightly altered and could not explain the high incidence of atrial arrhythmias in this model (5). Experimental CHF, too, causes discrete changes in atrial AP properties and currents (11).

In this study, we investigated in sheep the structural and functional effects of chronic dilation of the left atrium (LA) caused by a moderate volume overload by performing a left-right aorto-pulmonary artery shunt (APS) to increase flow in the pulmonary vein. One of the main advantages of this model is the creation of a fixed, reproducible volume overload in the LA that is readily abolished by clamping the prosthesis. The atrial appendage, which has been extensively used in the studies on mechanisms of AF, was also used here to follow histologic and cellular electrophysiologic changes during the development and reversion of the cardiopathy.

From the *CNRS-UMR-8078, Hôpital Marie-Lannelongue, Le Plessis-Robinson, France; †Institut Mutualiste Montsouris, Paris, France; ‡Hôpital Antoine Béclère, Clamart, France; and the §INSERM U-460, Hôpital Bichat and INSERM U-621, Université Pierre et Marie Curie, Paris, France. Supported by grants from the Fondation de l'Avenir, Societé Française de Cardiologie and Servier (E. Coraboeuf prize). Drs. Deroubaix and Folliguet contributed equally to this work.

Manuscript received May 28, 2004; revised manuscript received July 12, 2004, accepted July 29, 2004.

Abbreviations and Acronyms

AF = atrial fibrillation
AP = action potential
APS = aorto-pulmonary artery shunt
APSR = aorto-pulmonary artery shunt reversion
CHF = congestive heart failure
ERP = effective refractory period
I_{Ca} = L-type calcium current
LA = left atria/atrial
LAA = left atrial area
LV = left ventricle/ventricular
RAF = rapid atrial firing

METHODS

Surgical procedure. We studied 28 adult Ile-de-France sheep, with the approval of our ethics committee and in accordance with the "Guide for the Care and Use of Laboratory Animals" (National Research Council). Sheep were anesthetized with thiopental (10 mg/kg) followed by isoflurane in 100% oxygen and ventilated. Central anastomosis was performed between the thoracic descending aorta and the pulmonary artery trunk, using an 8-mm polytetrafluoroethylene tube (Gore-Tex; Gore, Flagstaff, Arizona). This procedure generated the classical hemodynamic pattern observed after systemic pulmonary shunt (12). The reversibility of the cardiopathy produced was studied by clamping the tube three to four months after its implantation. The animals were left to recover with the required analgesic regimen (morphine 0.5 mg/kg intramuscularly, twice daily, flunixin 1 mg/kg intramuscularly, once) and were maintained on aspirin (100 mg/day).

We studied animals in three experimental states: control state, three to four months after APS, and three to four months after shunt closure (aorto-pulmonary artery shunt reversion [APSR]). We checked the homogeneity of our animal population by carrying out clinical and echocardiographic examinations before any surgical intervention. We also checked the reproducibility of the model by echocardiography in the APS state (for the G2 and G3 groups). For histologic and cellular electrophysiologic studies, 10 animals were studied after sacrifice in the control state (G1), 12 in the APS state (G2), and the remaining 6 in the APSR state (G3).

Echocardiography. Transthoracic echocardiography was performed with a Vivid five echograph (General Electric Medical Systems Europe, Buc, France). In parasternal long-axis view, the left ventricular end-diastolic diameter (LVEDD) was defined as the largest left ventricle (LV) diameter; left ventricular end-systolic diameter (LVESD) was defined as the smallest LV diameter, and LV fractional shortening was calculated as: [(LVEDD − LVESD)/LVEDD] × 100. Mitral annulus diameter was defined as the distance between the insertion of the anterior and posterior mitral leaflets, and left atrial area (LAA) was measured by planimetry in systole. Linear dimensions and areas were normalized by weight$^{0.33}$ and by weight$^{0.66}$, respectively, according to allometry.

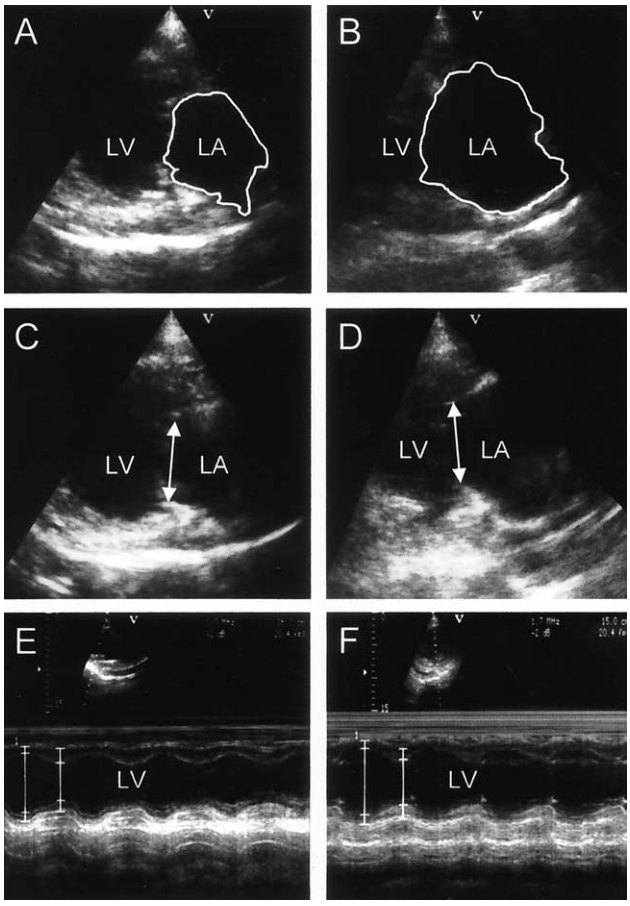

Figure 1. Two-dimensional echocardiographic images of left atrium (LA) **(A, B)** and the mitral annulus **(C, D)** in the control **(A, C)** and aorto-pulmonary artery shunt (APS) **(B, D)** states. Time-motion echocardiographic images of the left ventricle (LV) in the control **(E)** and APS **(F)** states.

Electrophysiologic testing. An electrocardiogram was recorded for 2 h in all anesthetized sheep in the three states to analyze the rhythm, to record atrial premature depolarization, and to compare the electrocardiographic characteristics between animals at the different stages. For electrophysiologic testing, a quadripolar electrode catheter was introduced percutaneously via the jugular vein and positioned under fluoroscopic guidance in the lateral or anterior free wall of the right atrium. Surface and intra-cardiac electrograms were recorded simultaneously. Suprathreshold stimulation was delivered in sinus rhythm and during stimulation at 600, 500, and 400 ms for measurement of the ERP, to trigger rapid atrial firing (RAF), defined as two or more successive atrial activations (13), or AF, which was considered to be sustained if it lasted longer than 1 min.

Histologic study. Tissue samples were fixed in 4% formaldehyde and embedded in paraffin. Sections (6 μm) were stained with Masson's trichrome. Myocyte diameter was determined by measuring the short axis of 150 randomly chosen cells per field (10 fields per animal). Myocytes were

Table 1. Echocardiographic Parameters

Group	G1 Control (n = 6)	G2 APS (n = 12)	G3 APSR (n = 6)
LAA (cm^2/m^2)	91.7 ± 10.4	146.2 ± 35.4*	86.8 ± 14.7
LVEDD (cm/m)	11.4 ± 1.2	12.0 ± 1.8	12.1 ± 1.3
LVESD (cm/m)	8.0 ± 0.6	8.3 ± 1.4	8.7 ± 1.0
MA (cm/m)	7.2 ± 0.7	7.6 ± 1.0	7.3 ± 1.0 (n = 5)
FS (%)	28.9 ± 6.3	30.4 ± 5.6	28.1 ± 4.8

Values are mean ± SD. *$p < 0.0001$ (vs. control).
APS = aorto-pulmonary artery shunt; APSR = aorto-pulmonary artery shunt reversion; FS = left ventricular fractional shortening; LAA = left atrial area; LVEDD = left ventricular end-diastolic diameter; LVESD = left ventricular end-systolic diameter; MA = mitral annulus; n = number of animals.

examined by two independent investigators and considered myolytic if >20% of the sarcomere was absent.

Cellular electrophysiologic studies. Action potentials were recorded with microelectrodes in a left appendage sample superfused with Tyrode solution (35 ± 0.5°C) gassed with a 95% O_2 to 5% CO_2 mixture (14). The tissue was electrically driven (2- to 3-ms pulses) at 1 Hz. We determined resting membrane potential, AP amplitude, AP duration at 50% and 90% repolarization, and maximum upstroke velocity of the AP.

The L-type calcium current (I_{Ca}) was recorded in enzymatically isolated atrial myocytes with the patch clamp technique (15). The amplitude of I_{Ca} elicited by 300-ms test pulses (0.2 Hz, at 22°C to 24°C) was the difference between peak current and the current measured at the end of the pulse and was divided by cell membrane capacitance to obtain current density in picoampere/picofarad (pA/pF).

Statistical analysis. Data are expressed as mean values ± SEM unless otherwise stated. States (control state, APS, APSR) were compared by one-way analysis of variance, including Scheffé test. For ERP, different states were compared in the same animal by one-way analysis of variance for repeated measures, including Scheffé test. When analysis of variance rejected the null hypothesis ($p < 0.05$), a Scheffé test was performed providing the p values indicated in the text, which were considered significant when <0.05. Frequencies were analyzed by means of the chi-square test.

RESULTS

Clinical, echocardiographic, and histologic characteristics of sheep in the APS state. During the post-surgery period, all animals gained weight and showed no clinical signs of CHF. We first checked that normalized echocardiographic data did not differ significantly between the three groups in the control state and between G2 and G3 in the APS state. Three to four months after surgery, the LAA of animals in the APS state had increased by approximately 50%, with no change in mitral annulus diameter and no mitral insufficiency detected (color Doppler). Moreover, the LV was not dilated, and its shortening fraction was normal (Fig. 1, Table 1).

Control tissue sections showed narrow myocytes well aligned and surrounded by little interstitial tissue. In dilated atria, myocytes were enlarged (18.7 ± 0.6 μm vs. 10.9 ± 0.4 μm in control sections, $p < 0.0001$) (Figs. 2A, 2B, and 2D), and 39.8% showed myolysis (Figs. 2E and 2F); there was no fibrosis (Fig. 2B).

Atrial vulnerability in the APS state. Prolonged electrocardiographic recording (2 h) performed in anesthetized sheep in the control and in the APS states showed no spontaneous episode of AF or atrial premature depolarization. Moreover, the electrocardiogram was unchanged between groups; notably the duration of the P wave was not significantly increased in the APS state (7.1 ± 0.5 ms vs. 7.8 ± 0.7 ms in the control and APS states, respectively). Thus, we evaluated atrial vulnerability by performing electrophysiologic testing with a stimulation protocol identical to that currently used in clinical practice. Mean ERP measured in sinus rhythm, at two sites of the right atria and during atrial pacing did not differ significantly between the control, APS, and APSR states in G3 animals (Fig. 3A). In only two of six animals studied in the control state was a short RAF, lasting less than five atrial electrograms, triggered by a single extra stimulus. In contrast, all but one of the animals in the APS state displayed RAF of 3 to 16 atrial electrograms (Fig. 3B), reproducibly induced by an extra stimulation delivered in a fixed coupling interval. Moreover, in two sheep, RAF degenerated into a sustained episode of AF (Fig. 3C). No prolonged or fragmented atrial activity was observed in the APS state. No attempt was made to trigger AF with a burst of rapid stimulation or multiple extra stimuli to prevent any acute modification of the cellular properties of the cells (16,17).

Cellular electrical properties of dilated atria. Four cellular responses were recorded in all LA appendages studied: 1) A-type AP had a characteristic plateau shape; 2) B-type AP was triangular in shape; and 3) C-type AP was of low amplitude, with a lower resting potential. Unexcitable myocytes were classified as D-type cells if they responded with a slow or no AP (Fig. 4). Statistical analysis of the characteristics of AP confirmed the existence of three types of AP (Table 2). Note the shorter duration of B-type than of A-type AP (Table 2). In the control state (G1), most (80%) of the AP was of the A-type, with only low proportions of B-, C-, or D-type AP (8%, 6%, and 5%, respectively) (Fig. 4B). In contrast, in the APS state (G2) the proportion of A-type AP decreased strongly (20%),

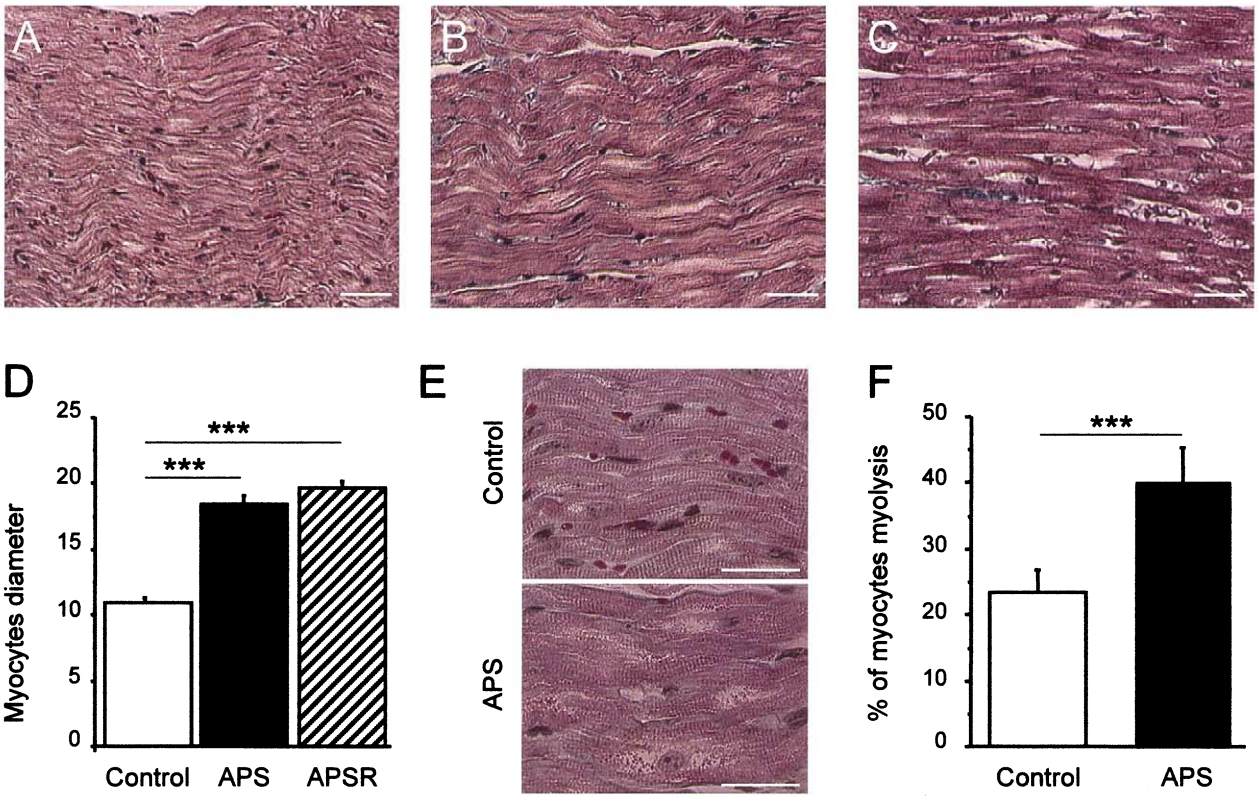

Figure 2. Tissue sections from LA after Masson's trichrome staining in the control **(A)**, aorto-pulmonary artery shunt (APS) **(B)**, and aorto-pulmonary artery shunt reversion (APSR) **(C)** states. **(D)** Myocyte diameters in the three groups of animals. Example of cell myolysis **(E)** and percentage of myolytic myocytes **(F)** in control and APS states. **Bar** = 40 μm; animal number = 9 (control state), 7 (APS), 6 (APSR). ***$p < 0.0001$.

whereas the proportions of B-type and C-type APs, together with D-type cells, increased to similar levels (20%, 25%, and 26%, respectively) (Fig. 4B). Furthermore, the percentage of D-type cells was correlated with LAA ($r^2 = 0.68$, $p < 0.01$) (Fig. 4C). Fewer AP were recorded in atrial appendages in APS than in the control state (270 vs. 380), reflecting the fact that the area of diseased samples that was stimulated by the surface electrode was limited compared with the robust stimulation of the whole control samples.

Downregulation of the L-type calcium current in dilated LA. We analyzed I_{Ca} as it is the main depolarizing current during the AP plateau phase which is reduced in APS. In atrial myocytes in the control and APS states, 10-mV incremental depolarizing pulses activated a typical I_{Ca} (Fig. 5B). However, current density was lower in the APS state (3.03 ± 0.23 pA/pF vs. 1.37 ± 0.14 pA/pF; $p < 0.001$). Membrane capacitance, which reflects cell size, was higher in the APS than in the control state (Fig. 5A). We then investigated whether changes in I_{Ca} phosphorylation contributed to current downregulation in the APS state. Isoproterenol (1 μM) stimulated I_{Ca} such that I_{Ca} density did not differ between myocytes in the control and APS states (Figs. 6A and 6B). Furthermore, isoproterenol activated the plateau phase and shortened the late repolarization phase of the B-type AP (five cells), an effect resembling that of isoproterenol on A-type AP (six cells) (Fig. 6C). In D-type cells, isoproterenol also restored an AP with a plateau phase (four cells) (Fig. 6C).

Partial reversibility of atrial remodeling after suppression of the shunt. The LAA was not different from control values after shunt suppression (Table 1). Histologic study showed that myocytes remained hypertrophied (19.7 ± 0.5 μm in the APSR state vs. 10.9 ± 0.4 μm in the control state; $p < 0.0001$) (Figs. 2C and 2D), and this was corroborated by the persistence of high membrane capacitance (Fig. 5B). Electrophysiologic testing showed rare RAF (one in six animals) and no AF episodes.

As in the control state, A-type AP predominated in the APSR state (63.4%) and rare B-type (17.6%) and C-type (10.9%) AP were observed, together with a few D-type cells (8%) (Fig. 4B). The characteristics of AP, regardless of the type of AP considered, did not differ between the control and APSR states (Table 2). Finally, I_{Ca} density was similar in myocytes from animals in the control and APSR states (Fig. 5A).

DISCUSSION

The original feature of the model described in this study is the creation of a chronic and moderate LA dilation without LV dysfunction and AF, resembling the cardiac status associated with moderate chronic mitral regurgitation (9). This contrasts with other models of dilated atria in which

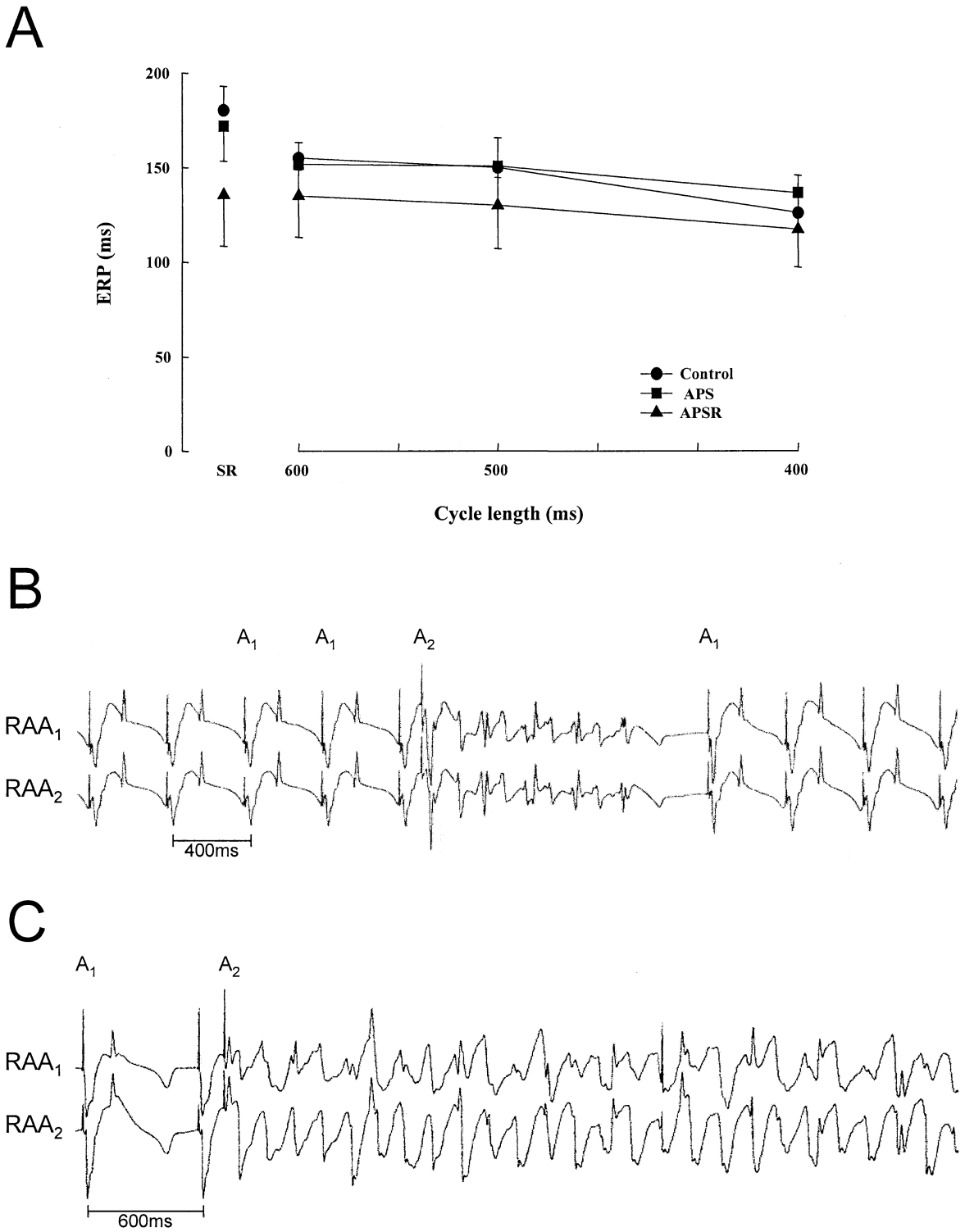

Figure 3. (A) Effective refractory period (ERP) measured in the right atrium during sinus rhythm (SR) and at various cycle lengths in the control, aorto-pulmonary artery shunt (APS), and aorto-pulmonary artery shunt reversion (APSR) states in six G3 animals. **(B)** Example of repetitive atrial firing and of **(C)** a sustained episode of atrial fibrillation triggered by a single extra beat in the APS state. A_1 (paced) and A_2 (premature) atrial electrograms. RAA_1 and RAA_2 = right atrial electrograms recorded with the quadripolar electrode.

there is frequently marked or acute atrial dilation, LV dysfunction, and AF (4–6,9). The three months elapsed since the implantation of an aorto-pulmonary shunt and the small shunt diameter probably accounted for the lack of cardiac consequences of high blood flow rates. Our main finding is that this clinically silent and moderate volume overload of the atria causes already marked changes in transmembrane AP and calcium current, together with

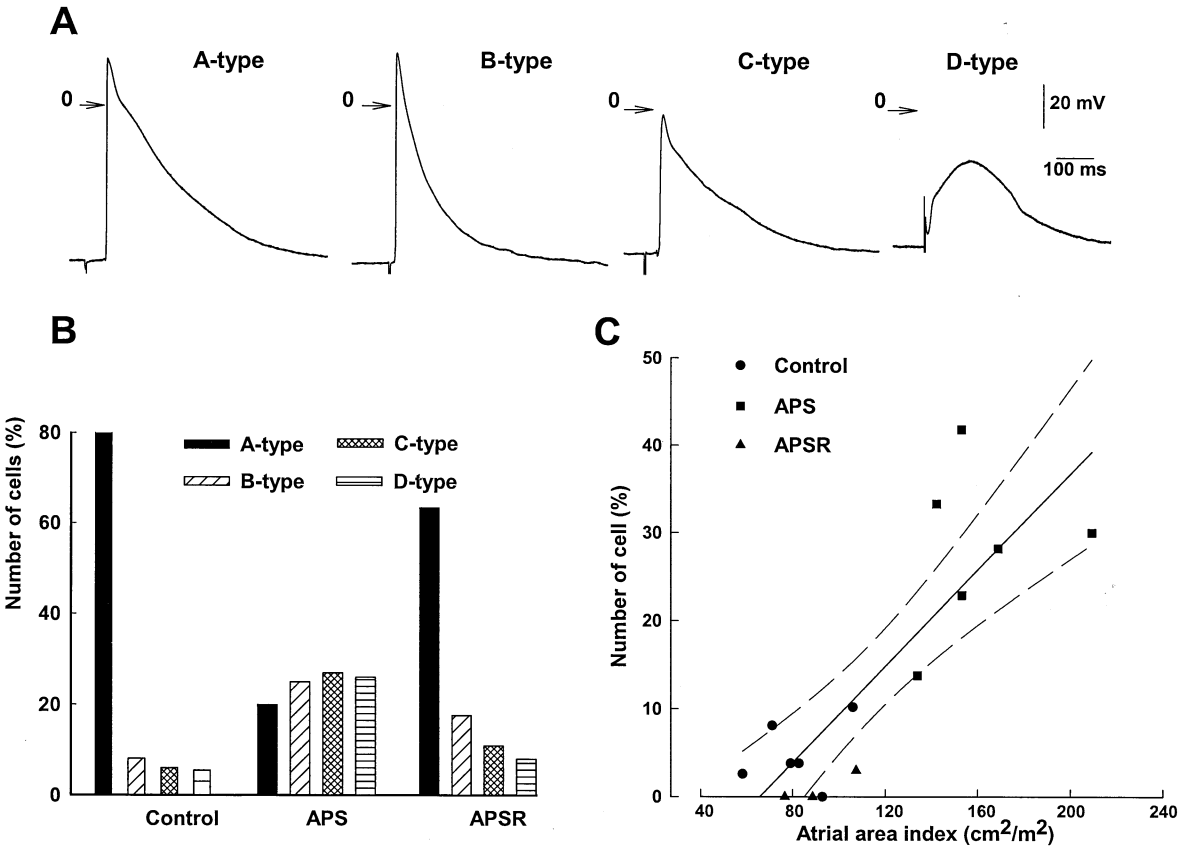

Figure 4. **(A)** Examples of the four types of action potential (AP) in the control state. **(B)** Distribution of the four types of AP recorded in the control, aorto-pulmonary artery shunt (APS), and aorto-pulmonary artery shunt reversion (APSR) states (numbers of animals: 7, 7, and 3, respectively; $p < 0.001$). **(C)** Correlation analysis of percent D-type cells as a function of atrial area index. **Solid line** = regression line; **dashed line** = 95% confidence interval.

some atrial vulnerability. These cellular alterations, which are known to contribute to the substrate of AF, were reversed on the normalization of atrial hemodynamic working conditions.

In dilated atria, the typical cardiac AP with a plateau phase was replaced by a triangular-shaped or slow-response AP. This resembles the changes in AP found in human atrial myocytes from patients in AF (10,18). Boutjdir et al. (18) found in right atrial preparations of patients in sinus rhythm, 77% of plateau phase and 23% of triangular AP, whereas during AF there was 97% of triangular-shaped AP and 15% of cells showed a slow response. In addition, many atrial myocytes of sheep in the APS state were unexcitable. Moreover, because of the difficulty to stimulate the whole preparation, a lower number of APs were recorded in trabeculae from dilated atria, suggesting altered electrical coupling. In dogs with mitral valve disease, <20% of the cells are unexcitable, whereas AP characteristics are similar to those in control dogs (5). We also found that mean AP duration (i.e. mean A-, B-, C-type AP duration) did not

Table 2. Left Atrial Action Potential Parameters in the Control, APS, and APSR States

Group	State (N)	Type (n)	Er (mV)	Ampl (mV)	Vmax (V/s)	APD (50%) (ms)	APD (90%) (ms)
G1	Control (7)	A (307)	−74.2 ± 2.0	86.1 ± 3.7	152.3 ± 48.4	69.7 ± 14.8	187.3 ± 22.4
		B (31)	−75.2 ± 5.0	87.2 ± 10.7	170.8 ± 59.1	42.1 ± 5.6‡	133.7 ± 16.1‡
		C (22)	−61.5 ± 5.1‡	56.6 ± 7.5§	61.4 ± 28.7‡	71.7 ± 11.3	193.0 ± 28.5
G2	APS (7)	A (53)	−67.1 ± 7.0†	69.6 ± 8.7*	130.5 ± 111.7	69.1 ± 29.1	189.6 ± 34.9
		B (64)	−69.8 ± 4.2	76.4 ± 8.9	204.3 ± 130.5	42.1 ± 15.5	160.5 ± 34.9
		C (79)	−66.5 ± 6.6	58.0 ± 10.2	132.8 ± 95.7	59.0 ± 20.4	167.1 ± 23.6
G3	APSR (3)	A (151)	−79.0 ± 1.7	88.3 ± 2.5	172.0 ± 59.2	66.0 ± 12.2	154.6 ± 25.4
		B (42)	−68.6 ± 9.6	78.9 ± 5.4	141.5 ± 60.0	45.0 ± 9.3	138.6 ± 6.3
		C (26)	−74.0 ± 3.2†	61.5 ± 4.2‡	132.9 ± 154.4	68.1 ± 20.0	169.9 ± 18.1

Values are mean ± SD. B-type or C-type versus A-type in G1, G2, or G3; ‡$p < 0.001$, §$p < 0.001$. A-, B-, or C-type action potential in APS or APSR state versus control state; †$p < 0.05$, *$p < 0.001$.

Ampl = action potential amplitude; APD (50%), APD (90%) = action potential duration at 50% and 90% repolarization; APS = aorto-pulmonary artery shunt; APSR = aorto-pulmonary artery shunt reversion; Er = resting membrane potential; N = number of animals; n = number of cells tested; Vmax = maximum rate of rise of the action potential.

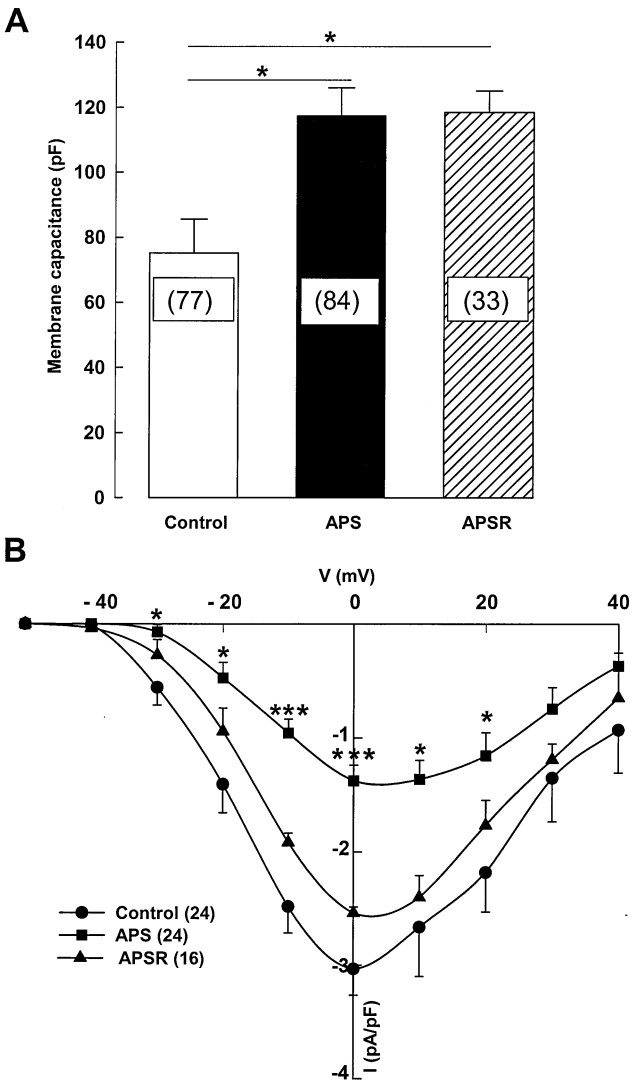

Figure 5. Membrane capacitance **(A)** and current density-voltage relationship **(B)** of atrial myocytes recorded in the control, aorto-pulmonary artery shunt (APS), and aorto-pulmonary artery shunt reversion (APSR) states. **Number in parentheses** = number of cells tested. The numbers of animals used for **A** and **B** were: controls (8, 7), APS (10, 8), and APSR (4, 3). $^{*}p < 0.05$; $^{***}p < 0.0001$.

differ significantly between the control and APS states. Thus, greater heterogeneity of the AP population appears to be an important feature of the electrical remodeling of dilated atria. Furthermore, the regions used to record AP (free wall in dogs [5], appendage in humans [10,18,19], and sheep atria) may account for the differences between studies. The fact that alterations of the cellular electrophysiologic properties are present in dilated LA of sheep in the APS state as well as during right atrial dilation in patients in sinus rhythm (10) suggests that they are an early event in the constitution of the AF substrate.

The short AP of diseased atria could be a result of changes of a number of ionic currents, but studies in animal models or in humans in the setting of AF have all pointed to a clear reduction in I_{Ca} (3,10,20,21). The mechanism responsible for the reduction in I_{Ca} is still a matter of debate (22). A decrease in the number of calcium channel alpha$_1$-subunits has been reported in the setting of AF both in animal models (21) and in humans (23). Changes in the regulation of I_{Ca} by second messengers have been reported during AF and hemodynamic overload of the atria (10,15,21). For instance, I_{Ca} is highly sensitive to beta-adrenergic stimulation in dilated and fibrillating human atria (10,20), and in the atria of rat in CHF (15). In cardiac myocytes, I_{Ca} is regulated by beta-adrenergic agonists through a cyclic adenosine monophosphate-dependent pathway that increases the availability and the probability of opening of the calcium channel. In addition, it has been shown that Ca^{2+} channels in cardiac myocytes are phosphorylated in the absence of any neurohormonal stimulation and that this basal phosphorylation is necessary to maintain normal channel function (24). The finding in our model of isolated and moderate LA dilation, that I_{Ca} is already reduced and highly responsive to beta-adrenergic agonists suggests that local factors are responsible for the current downregulation. For instance, during the volume overload of the atria, neurohormones or peptides could be locally secreted and in turn alter the phosphorylation of the atrial myocardium. Atrial natriuretic peptide that regulates intracellular cyclic adenosine monophosphate concentration and that accumulates in dilated or fibrillating atria (25) is one candidate. Moreover, we found that catecholamines restored atrial electrical activity as reported in humans (19) and in experimental models (5,6). Thus, the pharmacologic modulation of adrenergic pathways may be a potential target for therapy in the setting of dilated and hemodynamically overloaded atria.

Other currents are involved in the modification of AP during AF or in dilated atria (3,10,21). For instance, the voltage-gated outward potassium currents that are activated during the plateau phase are reduced in diseased human atria or in animal models of AF (10,21,26). Our observation that C-type AP became hyperpolarized in the APS state and reached significance in the APSR state suggests alterations of background currents as in human atrial appendage, where messenger ribonucleic acid of Kir2.1 and the background I_{K1} current are upregulated during AF, contributing to the more negative resting potential and shorter AP of AF than control myocytes (27). Clearly, studies focused on examining the regulation of repolarizing currents in volume-overloaded and vulnerable atria would be of great interest.

Changes in cellular electrophysiology and atrial vulnerability. Heterogeneity, AP shortening, and loss of excitability in the APS state are potentially proarrhythmic factors (28). Indeed, APS sheep clearly display signs of atrial vulnerability, such as the triggering of RAF, or more rarely AF episodes with a single premature stimulation, indicating a strong tendency of dilated atria to develop reentry (29). The normalization of atrial electrical properties, but not of cell hypertrophy, in the APSR

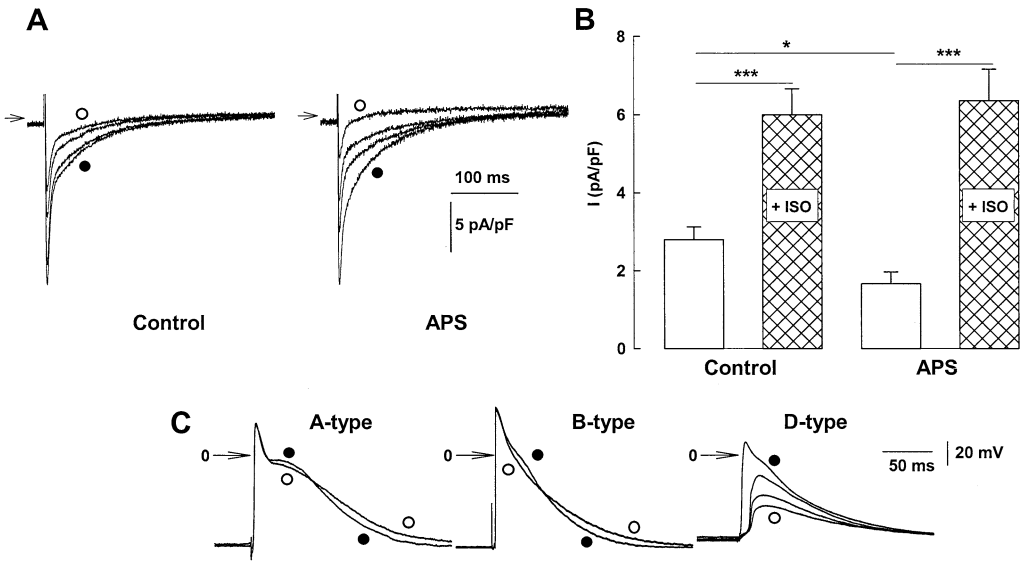

Figure 6. **(A)** Effect of isoproterenol (ISO) on I_{Ca} in control and aorto-pulmonary artery shunt (APS) states: initial **(open circles)** and steady-state effects of 1 μM isoproterenol **(solid circles)**. **(B)** Current densities before **(open bars)** and at steady state effects of isoproterenol (**hatched bars**, +ISO) in the control (19 cells from 7 animals) and APS (27 cells from 9 animals) states. *$p < 0.05$; ***$p < 0.0001$. **(C)** Effect of isoproterenol (**solid circles**, 4-min exposure) on A-type action potential (AP) in the control state, on B- and D-type AP in the APS state.

state also suggests a relationship between atrial vulnerability and AP alterations.

None of the animals in the APS state displayed spontaneous AF, and, once triggered, arrhythmia was rarely sustained, suggesting that atrial myocardial remodeling was not severe or that additional factors were lacking. In the model of mitral regurgitation in the dog, characterized by a marked atrial dilation and myocardial fibrosis, sustained AF can be induced by burst pacing in only 53% of dogs, suggesting a threshold to the extent of atrial pathology necessary for sustenance of AF (9). In our model, the structural abnormalities were limited to myocyte hypertrophy and myolysis, without fibrosis, and may be insufficient for the activation of sustained AF. Moreover, in our study we did not attempt to trigger long episodes of AF using rapid atrial pacing (30) to prevent any acute alterations of cellular electrophysiology (16,17). Overall, these results indicate that cellular electrical abnormalities in volume-overloaded LA may contribute to atrial vulnerability but are insufficient for spontaneous or sustained AF (31). During CHF, despite the normalization of electrical properties, atria remain vulnerable to AF, demonstrating the role of myocardial structural remodeling in this clinical setting (32).

Study limitations. First, as we studied only the left appendage, the extent of cellular electrophysiologic alterations in dilated sheep atria is unknown. Most other studies on the substrate of atrial arrhythmia have also been performed on the atrial appendage, which undergoes marked structural and functional remodeling during AF. We observed no change in ERP in our model, as previously reported (33), whereas ERP is shortened during acute atrial dilation (4,34) or prolonged in the dog model of mitral regurgitation and during CHF in humans (9,35). It is possible that neither the level nor the duration of pressure overload in our model was sufficient to induce changes in ERP (4). As ERP was determined only in the right atrium, no information is available concerning the possible dispersion of ERP, which has been shown to be proarrhythmic for AF. However, in the dog with mitral regurgitation there is no dispersion of ERP.

Conclusions. We demonstrate here that a moderate atrial volume overload without apparent clinical consequence causes already profound changes in the electrophysiologic properties of the atrial myocardium resembling those observed during AF and probably contributing to atrial vulnerability. This study may have clinical implications for the development of a rationale for early clinical intervention to normalize atrial hemodynamic loading conditions, for example, in mitral valve disease.

Acknowledgments

We thank Dr. Patrice Dervanian for helpful discussion and suggestions and the surgical team of IMM Recherche for their excellent technical assistance.

Reprint requests and correspondence: Dr. Stéphane N. Hatem, INSERM U-460, Medical Hospital Bichat, 46 rue Henri Huchard, 75018 Paris, France. E-mail: Stephane.Hatem@bichat.inserm.fr.

REFERENCES

1. Benjamin EJ, Levy D, Vaziri SM, D'Agostino RB, Belanger AJ, Wolf PA. Independent risk factors for atrial fibrillation in a population-based cohort: the Framingham Heart Study. JAMA 1994;271:840–4.
2. Henri WL, Morganroth J, Pearlman AS, et al. Relation between echocardiographically determined left atrial size and atrial fibrillation. Circulation 1976;53:273–9.

3. Nattel S, Li D, Yue L. Basic mechanisms of atrial fibrillation: very new insights into very old ideas. Annu Rev Physiol 2000;62:51–77.
4. Ravelli F, Allessie M. Effects of atrial dilatation on refractory period and vulnerability to atrial fibrillation in the isolated Langendorff-perfused rabbit heart. Circulation 1997;96:1686–95.
5. Boyden PA, Tilley LP, Pham TD, Liu S-K, Fenoglio JJ Jr., Wit AL. Effects of left atrial enlargement on atrial transmembrane potentials and structure in dogs with mitral valve fibrosis. Am J Cardiol 1982;49:1896–908.
6. Boyden PA, Tilley LP, Albala A, Liu S-K, Fenoglio JJ Jr., Wit AL. Mechanisms for atrial arrhythmias associated with cardiomyopathy: a study of feline hearts with primary myocardial disease. Circulation 1984;69:1036–47.
7. Wijffels MC, Kirchhof CJ, Dorland R, Allessie MA. Atrial fibrillation begets atrial fibrillation: a study in awake chronically instrumented goats. Circulation 1995;92:1954–68.
8. Everett TH IV, Li H, Mangrum JM, et al. Electrical, morphological and ultrastructural remodeling and reverse remodeling in a canine model of chronic atrial fibrillation. Circulation 2000;102:1454–60.
9. Verheule S, Wilson E, Everett T IV, Shanbhag S, Golden C, Olgin J. Alterations in atrial electrophysiology and tissue structure in a canine model of chronic atrial dilatation due to mitral regurgitation. Circulation 2003;107:2615–22.
10. Le Grand BL, Hatem S, Deroubaix E, Couetil JP, Coraboeuf E. Depressed transient outward and calcium currents in dilated human atria. Cardiovasc Res 1994;28:548–56.
11. Li D, Melnyk P, Feng J, et al. Effects of experimental heart failure on atrial cellular and ionic electrophysiology. Circulation 2000;101: 2631–8.
12. Senzaki H, Masutani S, Kobayashi J, et al. Ventricular afterload and ventricular work in Fontan circulation: comparison with normal two-ventricle circulation and single-ventricle circulation with Blalock-Taussig shunts. Circulation 2002;105:2885–92.
13. Hashiba K, Tanigawa M, Fukatani M, et al. Electrophysiologic properties of atrial muscle in paroxysmal atrial fibrillation. Am J Cardiol 1989;64:20J–3J.
14. Bru-Mercier G, Deroubaix E, Rousseau D, Coulombe A, Renaud J-F. Depressed transient outward potassium current density in catecholamine-depleted rat myocytes. Am J Physiol 2002;282:H1237–47.
15. Boixel C, Gonzalez W, Louedec L, Hatem SN. Mechanisms of L-type Ca^{2+} current downregulation in rat atrial myocytes during heart failure. Circ Res 2001;89:607–13.
16. Daoud EG, Bogun F, Goyal R, et al. Effect of atrial fibrillation on atrial refractoriness in humans. Circulation 1996;94:1600–6.
17. Goette A, Honeycutt C, Langberg JJ. Arrhythmias/pacing: electrical remodeling in atrial fibrillation. Time course and mechanisms. Circulation 1996;94:2968–74.
18. Boutjdir M, Le Heuzey JY, Lavergne T, et al. Inhomogeneity of cellular refractoriness in human atrium: factor of arrhythmia? Pacing Clin Electrophysiol 1986;9:1095–100.
19. Gelband H, Rosen MR, Myerburg RJ, Bush HL, Bassett AL, Hoffman BF. Restorative effect of epinephrine on the electrophysiologic properties of depressed human atrial tissue. J Electrocardiol 1977;10:313–20.
20. Van Wagoner DR, Pond AL, Lamorgesse M, Rossie SS, Mc Carty PM, Nerbonne JM. Atrial L-type Ca^{2+} currents and human atrial fibrillation. Circ Res 1999;85:428–36.
21. Yue L, Feng J, Gaspo R, Li GR, Wang Z, Nattel S. Ionic remodeling underlying action potential changes in a canine model of atrial fibrillation. Circ Res 1997;81:512–25.
22. Schotten U, Haase H, Frechen D, et al. The L-type Ca^{2+}-channel subunits α_{1C} and β_2 are not downregulated in atrial myocardium of patients with chronic atrial fibrillation. J Mol Cell Cardiol 2003;35: 437–43.
23. Lai LP, Su MJ, Lin JL, et al. Down-regulation of L-type calcium channel and sarcoplasmic reticular Ca^{2+}-ATPase mRNA in human atrial fibrillation without significant change in the mRNA of ryanodine receptor, calsequestrin and phospholamban: an insight into the mechanism of atrial electrical remodeling. J Am Coll Cardiol 1999;33: 1231–7.
24. Ono K, Fozzard HA. Phosphorylation restores activity of L-type calcium channels after rundown in inside-out patches from rabbit cardiac cells. J Physiol 1992;454:673–88.
25. Rossi A, Enriquez-Sarano M, Burnett JC, Lerman A, Abel MD, Seward JB. Natriuretic peptide levels in atrial fibrillation: a prospective hormonal and Doppler-echocardiographic study. J Am Coll Cardiol 2000;35:1256–62.
26. Van Wagoner DR, Pond AL, McCarty PM, Trimmer JS, Nerbonne JM. Outward K^+ current densities and Kv1.5 expression are reduced in chronic human atrial fibrillation. Circ Res 1997;80:772–81.
27. Dobrev D, Graf E, Wettwer E, et al. Molecular basis of downregulation of G-protein-coupled inward rectifying K^+ current I(K,ACh) in chronic human atrial fibrillation: decrease in GIRK4 mRNA correlates with shortening of action potentials. Circulation 2001;104:2551–7.
28. Allessie MA, Bonke FIM, Schopman FJG. Circus movement in rabbit atrial muscle as a mechanism of tachycardia. III. The "leading circle" concept: a new model of circus movement in cardiac tissue without involvement of an anatomical obstacle. Circ Res 1977;41:9–18.
29. Coumel P. Supraventricular tachycardia. In: Krikler DM, Goodwin JF, editors. Cardiac Arrhythmias: The Modern Electrophysiological Approach. Philadelphia, PA: WB Saunders, 1975;116–40.
30. Friedman HS, Sinha B, Tun A, Pasha R, Sharafkhaneh A, Bharadwaj A. Zones of atrial vulnerability: relationships to basic cycle length. Circulation 1996;94:1456–64.
31. Ausma J, Wijffels M, Thone F, Wouters L, Allessie M, Borgers M. Structural changes of atrial myocardium due to sustained atrial fibrillation in the goat. Circulation 1997;96:3157–63.
32. Cha TJ, Ehrlich JR, Zhang L, et al. Dissociation between ionic remodeling and ability to sustain atrial fibrillation during recovery from experimental congestive heart failure. Circulation 2004;109:412–8.
33. Wijffels MCEF, Kirchhof CJHJ, Dorland R, Power JBVS, Allessie MA. Electrical remodeling due to atrial fibrillation in chronically instrumented conscious goats: roles of neurohumoral change: ischemia, atrial stretch, and high rate of electrical activation. Circulation 1997; 96:3710–20.
34. Solti F, Vecsey T, Kékesi V, Juhász-Nagy A. The effect of atrial dilatation on the genesis of atrial arrhythmias. Cardiovasc Res 1989; 23:882–6.
35. Sanders P, Morton JB, Davidson NC, et al. Electrical remodeling of the atria in congestive heart failure: electrophysiological and electroanatomic mapping in humans. Circulation 2003;108:1461–8.